The Corner of the Equivalence Principle No Experiment Has Touched

Brecht Corbeel
Absolute Digital Publishers
absolutedigitalpublishers.com

September 20, 2026

Abstract. What exactly has been tested when we say the equivalence principle survives? Parametrizing the gravitational mass of a quantum system as an operator, weak-EP tests decompose into five logically independent components: classical-body universality, internal-state (diagonal) universality, internal-coherence (off-diagonal) universality, spatial-superposition universality, and entangled-state universality — the last asking whether a *nonseparable* state of two species falls universally, a question no combination of separable-state experiments can answer (we prove this in the mass-operator model). Auditing the published record against the basis — MICROSCOPE at 10^{-15}, dual-species drops at 10^{-12}, internal-superposition drops, clock redshift comparisons, antihydrogen — fills four columns and leaves the fifth empty. One buildable experiment reaches it: a dual-species interferometer operating on an entangled joint state, whose projected sensitivity we derive from demonstrated entangled-interferometry parameters, with the leading systematics and their mitigations each carried with a verified magnitude. We position the design against the one prior proposal in this direction found by our audit, state which theory classes predict a violation visible only in the empty column, and give the falsifiers.

Keywords: equivalence principle; universality of free fall; quantum tests; entangled interferometry; MICROSCOPE; atom interferometry; violation-operator basis.
Series: The Quantum–Relativity Papers, No. 9.

1 The equivalence principle has only ever been tested on separable states

The weak equivalence principle is among the most stringently confirmed statements in physics. The MICROSCOPE satellite bounds the Eötvös parameter of a titanium–platinum pair at $\eta(\mathrm{Ti},\mathrm{Pt}) = [-1.5 \pm 2.3\,(\mathrm{stat}) \pm 1.5\,(\mathrm{sys})] \times 10^{-15}$ [77], and light-pulse atom interferometry compares two rubidium isotopes in free fall at $\eta = [1.6 \pm 1.8\,(\mathrm{stat}) \pm 3.4\,(\mathrm{sys})] \times 10^{-12}$ [7]. What we ask here is not whether those bounds hold — they do — but what physical object each of them constrains. A torsion balance weighs one alloy against another. A dual-species interferometer drops two atomic clouds side by side. A clock-redshift comparison reads one worldline against another. In every case the falling system occupies a *separable* state: a definite classical body, a single quantum system, or a product of independently prepared single-species states. Nothing in the published record has dropped a *nonseparable* state of two species and asked whether that state falls universally. Whether the omission is a genuine gap or a triviality is the entire content of what follows.

That the distinction can matter at all is the lesson of Zych and Brukner [88]: the validity of the classical Einstein equivalence principle does not imply the validity of its quantum formulation, which "requires an independent experimental verification," because the quantum statement demands equivalence of the rest, inertial, and gravitational internal-energy *operators* and not merely of their expectation values. We take that operator-level requirement literally. Writing the rest mass-energy operator as $\hat{M} = m\,(1 + H_{\mathrm{int}}/mc^2)$ with H_{int} the internal Hamiltonian [89], and the gravitational mass as $m_g = m_i\,(1 + \hat{\eta})$, the equivalence principle for a quantum system is the statement $\hat{\eta} = 0$ as an operator. Classical universality of free fall is the vanishing of the scalar part of $\hat{\eta}$ alone; every genuinely quantum way the principle could fail is a structural feature of $\hat{\eta}$ on the internal — and, for two bodies, the joint — Hilbert space. The question "what has been tested?" becomes "which matrix elements of $\hat{\eta}$ has the record actually bounded?"

Expanded to second order in H_{int}/mc^2 and to two bodies, $\hat{\eta}$ carries exactly five kinds of matrix element, and we label them η_{cl} (a state-independent scalar), η_{diag} (diagonal in the internal energy basis), η_{coh} (off-diagonal in that basis), η_{sup} (dependence on the external spatial state beyond first order), and η_{ent} (the nonseparable two-body part). The first contribution of this paper, made precise as Proposition 1 and exact at the stated order, is that these five exhaust $\hat{\eta}$ at that order and are pairwise logically independent: for each pair there is a model in the declared class with one component nonzero and the other zero (Appendix A). The components themselves are not new — each has been written down, in one notation or another, by the authors we cite below — so the exhaustiveness-and-independence packaging is what we add, and its wording is gated, deliberately, by the novelty audit reported later in this section.

The scaffolding is inherited and we name its owners. The violation-operator formulation of the equivalence principle for quantum systems is Zych and Brukner's [88]; the mass-energy operator in interferometry is Zych et al.'s [89]; the extension to superposed spacetimes and quantum reference frames is Giacomini and Brukner's [? ?]. The classical parametrization descends from the Schiff conjecture that any theory sensitive to a weak-equivalence violation also violates local Lorentz and position invariance [64], and from Damour's account of the equivalence principle as a statement about the constancy of the coupling "constants" of physics [21]. The measurements are their authors', cited at their numbers in §3.

Because the fifth component invites an overclaim, we audited the literature for prior proposals to test free fall on an entangled state, and two are genuine. Geiger and Trupke [34] proposed a differential $^{85}\mathrm{Rb}/^{87}\mathrm{Rb}$ interferometer operating on a heralded-single-photon entangled joint state, projecting an Eötvös accuracy below 10^{-7} — and a decade of entangled-atom metrology has grown up alongside the proposal. Bose et al. [14] defined an "entanglement-entropy" weak equivalence principle on the gravitationally self-entangling two-mass platform, bounding a single common mass ratio rather than a two-species differential. A third proposal, Cepollaro and Giacomini [15], uses entangled clocks, but as a resource for the quantum-reference-frame transform of one delocalized clock's proper time rather than as an independent two-species free-fall observable, a difference we argue explicitly in Appendix B. We therefore do *not* claim the first entangled-state equivalence-principle test: the experimental idea is Geiger and Trupke's, and we say so wherever the design of §5 appears.

What remains ours is narrower and, we will argue, sharper. First, we audit the published record against the basis, assigning every bound to the component combination it constrains, with the compilation in §4 (Fig. 1, Table 1). Second, we prove, exactly within the model class, that no set of measurements on separable states can bound η_{ent} (Theorem 5.1) — which is precisely the theoretical connection Geiger and Trupke noted was missing when they wrote that "there is currently no theoretical model which addresses the question whether or not the presence of entanglement in a system would result in a violation of the WEP." Third, we give a design envelope (structured, its inputs verified) for a dual-species entangled interferometer, deriving its projected η_{ent} reach from demonstrated entangled-interferometry parameters and stating where it improves on Geiger and Trupke's 10^{-7}-class projection and where it does not.

Section 2 builds the basis and sketches the independence models; §3 narrates the record, each entry at its number; §4 performs the audit and exhibits the empty column; §5 states the independence theorem and the one experiment that defeats it; and §6 maps which theory classes place a violation in the empty column, tying the corner to the gravitationally-induced-entanglement debate [18] and to the clock-redshift lineage [17] of this series. The claim throughout is not that the corner hides a violation — we expect it does not — but that "the equivalence principle survives" is, read precisely, a statement about four components, and the fifth has never been in the apparatus.

2 The violation operator has five components at second order, and they are pairwise independent

The value of an operator formulation is that it forces a bookkeeping the expectation-value statement of the equivalence principle hides. If gravitational mass equals inertial mass only on average, a system can satisfy $\langle\hat{\eta}\rangle = 0$ in every state that has ever fallen and still carry a nonzero $\hat{\eta}$ whose signature appears only in states no one has prepared. To make "which states" a finite question we classify the matrix elements of $\hat{\eta}$ rather than its expectation values, and the classification closes after five entries once the order in H_{int}/mc^2 and the number of bodies are fixed.

Proposition 1 (The five-component basis; ours as packaging, exact at the stated order)**.** *Model the rest mass-energy of a system as the operator $\hat{M} = m\,(1+H_{\mathrm{int}}/mc^2)$ on the internal Hilbert space, and its gravitational coupling as $m_g = m_i\,(1+\hat{\eta})$, where $\hat{\eta}$ is an operator on the internal and, for multipartite tests, the joint Hilbert space. Expanded to second order in H_{int}/mc^2 and to two bodies A and B,*

$$\begin{aligned}\hat{\eta} \;=\; \eta_{\mathrm{cl}}\,\mathbf{1} \;+\; \sum_n \eta^{(n)}_{\mathrm{diag}}\,\Pi_n \;+\; \sum_{m\neq n} \eta^{(mn)}_{\mathrm{coh}}\,|m\rangle\langle n| \\ +\; \hat{\eta}_{\mathrm{sup}}(\hat{X},\hat{P}) \;+\; \hat{\eta}_{\mathrm{ent}},\end{aligned} \tag{1}$$

where (i) η_{cl} is a state-independent scalar (classical universality of free fall); (ii) $\eta^{(n)}_{\mathrm{diag}}$ is diagonal in the internal energy eigenbasis $\{|n\rangle\}$ with projectors $\Pi_n = |n\rangle\langle n|$, a state-dependent free-fall rate constrained by clock/redshift and internal-state drop tests; (iii) $\eta^{(mn)}_{\mathrm{coh}}$ is off-diagonal, coupling internal coherences to free fall and bounded by internal-superposition drops if *the interferometric phases are read, which the audit decides;*

(iv) $\hat{\eta}_{\rm sup}(\hat{X},\hat{P})$ depends on the external spatial state beyond first order, the spatial-superposition and gravitational Aharonov–Bohm class; and (v) $\hat{\eta}_{\rm ent}$ is the nonseparable two-body part, defined by $\langle\hat{\eta}_{AB}\rangle \neq \langle\hat{\eta}_A\rangle + \langle\hat{\eta}_B\rangle$ on entangled states of A and B. Within the declared model class these five exhaust $\hat{\eta}$ at the stated order, and they are pairwise independent: for each pair, Appendix A exhibits a model in the class with one component nonzero and the other zero.

The decomposition earns the word "basis" only if two claims hold, and they carry different grades. Exhaustiveness — that Eq. (1) has no sixth term — is exact, but exact *within a declared class*: we fix the coupling to be at most quadratic in $H_{\rm int}/mc^2$, linear in the two-body correlation, and analytic in the external phase-space operators, and we state that limitation here rather than in a footnote because it is where the claim could be attacked. A cubic internal coupling or a three-body correlation would add terms; the audit and the experiment both live at an order where those are below any foreseeable sensitivity, so the class is the right one for reading the record, not a universal truth about $\hat{\eta}$. Pairwise independence, by contrast, is a constructive model-theoretic fact (Appendix A) and inherits no such caveat: it says the five knobs can be turned separately, so a bound on one is silent about the others unless a further assumption ties them.

Each component sits at a definite distance from Zych and Brukner's original requirement, and naming the distance is how the packaging avoids paraphrasing them loosely. Their quantum Einstein equivalence principle demands equality of the rest, inertial, and gravitational internal-energy operators [88]; $\eta_{\rm cl}$ is the part of a violation that survives even when $H_{\rm int}$ is a c-number, i.e. the only part a body with no relevant internal structure can carry, and it is exactly the classical Eötvös parameter that torsion balances and MICROSCOPE bound [65, 77]. The diagonal component $\eta_{\rm diag}$ is the leading operator-level term: it makes the free-fall rate depend on which internal energy eigenstate the system is in, so it is the component a clock reads as an anomalous redshift and an internal-state drop reads as a state-dependent g. That a clock in superposition of energies loses interferometric visibility to differential proper time — the mechanism Zych et al. identified [89] — is the observable through which $\eta_{\rm diag}$ and its off-diagonal partner become distinguishable at all.

The off-diagonal component $\eta_{\rm coh}$ is where the audit will do its most delicate work, and the model shows why. A drop of an atom prepared in a coherent superposition of two internal energy eigenstates is sensitive to $\eta_{\rm coh}^{(mn)}$ only through the relative phase of the returning arms; a measurement that reads only populations bounds $\eta_{\rm diag}$ and is blind to $\eta_{\rm coh}$, while a measurement that reads the phase bounds a specific combination of the two. Rosi et al.'s test of the equivalence principle for rubidium in a superposition of hyperfine states reached a relative uncertainty in the low 10^{-9} [61], and whether that bound touches $\eta_{\rm coh}$ or only $\eta_{\rm diag}$ turns entirely on which quantity the gradiometer read — the kind of observable-to-component question the audit resolves case by case in Appendix B, not by fiat here. That a free fall induces a mass-independent phase shift and a dephasing of the internal state, as Anastopoulos and Hu showed within a model [4], and that gravitational time dilation decoheres a composite body's centre of mass through its own internal clock [59], are the two mechanisms that populate the off-diagonal sector in concrete theories; both act on one body, and neither reaches $\eta_{\rm ent}$.

The spatial component $\hat{\eta}_{\rm sup}(\hat{X},\hat{P})$ is the first to leave the internal Hilbert space. It collects any dependence of free fall on the external state beyond the uniform-field, first-order term — the regime where a wavepacket's finite extent or a genuine spatial superposition matters. Seveso and Paris found, within a Fisher-information formulation, that quantum probes satisfy the weak equivalence principle exactly in a uniform field but that "gravity gradients can violate this principle" [69], which is precisely the statement that $\hat{\eta}_{\rm sup}$ is a gradient-order effect; the gravitational Aharonov–Bohm measurement of Overstreet et al. [54] and the effective-inertial-frame technique that suppresses gradient systematics to below one part in 10^{13} [53] are the experiments that live nearest this component. We grade the identification of $\hat{\eta}_{\rm sup}$ with the gravitational Aharonov–Bohm observable as structured rather than exact: the mapping is a leading-order reading of the phase, and the translation algebra that makes it precise, together with its cross terms against $\eta_{\rm diag}$, is carried in Appendix B.

The fifth component is the one the rest of the paper is about, and Eq. (1) states its definition rather than derives it: $\hat{\eta}_{\rm ent}$ is whatever part of the two-body coupling fails to be the sum of the parts, so that $\langle\hat{\eta}_{AB}\rangle \neq \langle\hat{\eta}_A\rangle + \langle\hat{\eta}_B\rangle$ on a nonseparable state. On any product state the definition forces $\langle\hat{\eta}_{AB}\rangle = \langle\hat{\eta}_A\rangle + \langle\hat{\eta}_B\rangle$ identically, which is already the seed of the independence theorem of §5: the component is constructed to vanish from the statistics of exactly the states the record has measured. It is not an artifact of the parametrization. A nonlinear modification of quantum mechanics, in which the Hamiltonian depends on the state, generically makes an entangled pair evolve differently from any product, so $\hat{\eta}_{\rm ent} \neq 0$ is what a Weinberg-type nonlinearity would look like in free fall [83]; a semiclassical sourcing of gravity from the mean field of the joint state does the same [86]. Whether any such theory survives the no-signaling constraint is the subject of §6; here it is enough that the component is populated by real theories and not by algebra alone.

Two of the components are forced nonzero by explicit models, which is what keeps the basis from being a mere change of variables. Emelyanov's analysis of free fall in quantum field theory finds that "free-fall universality and the wave-packet spreading are mutually exclusive" [28], so a theory in which the spread of the wavepacket is more fundamental than the equivalence principle forces $\hat{\eta}_{\rm sup}$ nonzero by construction — the external-state dependence is not optional in such a model. In the opposite direction, Marletto and Vedral's reading of the equivalence principle as a gauge principle detecting the gravitational t^3 phase [48] locates the diagonal component in a concrete, and now measured, observable: the cubic-in-time phase a single species accrues in free fall, whose recent interferometric confirmation we take up in §3. That the framework Zych and Brukner built to expose the operator-level content of the principle also yields models with definite nonzero components [88] is why we treat the decomposition of $\hat{\eta}$ as physics rather than notation. The two claims of exhaustiveness that could still be attacked are the cross terms: the class of Definition 1 carries products such as $\eta_{\rm diag}\,\eta_{\rm sup}$ at the same order, and we keep those cross terms in the appendix rather than the display, stating here only that they do not add a sixth component — they mix existing ones, and the audit reports any cell whose assignment a cross term makes conditional.

The pairwise-independence claim is what makes the five labels a decomposition rather than a list, and two of its ten cases are worth sketching before the appendix proves all of them. A model with $\eta_{\rm cl} = 0$ but $\eta_{\rm diag} \neq 0$ is any dilaton coupling whose charge is an internal-energy-dependent quantity, so that a body's free fall depends on its internal state while a state-averaged Eötvös measurement returns zero [22]; a model with $\eta_{\rm diag} = \eta_{\rm coh} = 0$ but $\eta_{\rm ent} \neq 0$ is a two-body coupling that is a pure correlation, vanishing on every single-body reduced state — the explicit construction is Appendix A's Lemma 2. Because each such model lies in the declared class, no chain of reasoning internal to the class can derive one component from another, and in particular no amount of single-body precision can be leveraged into a statement about the joint one. That is the structural fact the audit turns into a picture and the experiment turns into a target.

3 Every bound in the record is a measurement on a separable state, and each carries its own number

The record of weak-equivalence tests is usually read as a single quantity improving over time, from Galileo's inclined plane through Eötvös to a satellite. Read through the basis of §2 it is instead four separate quantities, each improving on its own schedule, and one that has never been measured. Before the audit assigns bounds to components we make the structural observation that lets it: every entry below, without exception, is a measurement of $\langle\hat{\eta}\rangle$ in a separable state of the test system.

Proposition 2 (The record is separable-state data; ours as observation)**.** *Within the model class of Proposition 1, every published weak-equivalence bound — classical torsion-balance and space tests, dual-species and internal-state atom interferometry, clock-redshift comparisons, lunar laser ranging, and antimatter free fall — is a constraint on $\langle\hat{\eta}\rangle$ evaluated in a state that is separable across the two test species (a definite classical body, a single quantum system, or a product of independently prepared single-species states, internal superpositions included). Equivalently, the record is a function of $\{\eta_{\rm cl}, \eta_{\rm diag}, \eta_{\rm coh}, \eta_{\rm sup}\}$ alone. No entry is a measurement on a nonseparable two-species state.*

The classical column is the deepest. Rotating torsion balances at the Eöt-Wash scale reach the part-in-10^{13} level [82], with the beryllium–titanium differential acceleration measured at $\Delta a(\mathrm{Be,Ti}) = (0.6 \pm 3.1) \times 10^{-15}$ $\mathrm{m\,s^{-2}}$, an Eötvös parameter $\eta(\mathrm{Be,Ti}) = (0.3 \pm 1.8) \times 10^{-13}$ [65]; the Eöt-Wash program treats these balances as a low-energy frontier for new-force searches [2], and the pre-quantum confrontation of general relativity with experiment that frames the whole classical audit is Will's [84]. MICROSCOPE improved on the best ground result by nearly two orders of magnitude, from its first-data limit at the 10^{-15} level [76] to a final titanium–platinum bound $\eta(\mathrm{Ti,Pt}) = [-1.5 \pm 2.3\,(\mathrm{stat}) \pm 1.5\,(\mathrm{sys})] \times 10^{-15}$ combining to a limit of 2.7×10^{-15} [77, 78]. Lunar laser ranging adds a body of astronomical scale: the Earth–Moon system tests the equivalence principle at $\Delta(M_G/M_I)_{\rm EP} = (-1.0 \pm 1.4) \times 10^{-13}$ [85], refined against the INPOP17a ephemeris to $(-3.8 \pm 7.1) \times 10^{-14}$ [81], and it carries the Nordtvedt-effect constraint on the composition-dependence of self-gravitational energy that Nordtvedt's lineage first parametrized [51]. All of these bound $\eta_{\rm cl}$: the falling objects have no coherently prepared internal degree of freedom in play.

The same classical bounds are also read as fifth-force limits, and that reading shows what the deep classical column actually excludes. MICROSCOPE's null constrains a light-scalar dilaton coupling to baryon number below $|\alpha| < 10^{-11}$ [11], and the relative strength of a new long-range force below 3.2×10^{-11} for baryon number and 2.3×10^{-13} for the lepton-number combination [31]. In the basis of §2 these are bounds on $\eta_{\rm cl}$ and, through the composition dependence of the coupling, $\eta_{\rm diag}$ — exactly the columns a dilaton would populate, and their depth is why §6 can argue that a violation confined to the entangled column cannot be a dilaton.

Dual-species atom interferometry is where the record becomes explicitly quantum, and where the separability is easiest to miss because two species are present at once. Its own root is the single-species atomic-fountain gravimeter read against a falling corner cube [57], and the first genuine equivalence test in the family is Fray et al.'s $^{85}\mathrm{Rb}/^{87}\mathrm{Rb}$ comparison, which reached $\Delta g/g =$

$(1.2 \pm 1.7) \times 10^{-7}$ for the isotope pair and, in the same apparatus, $(0.4 \pm 1.2) \times 10^{-7}$ for two hyperfine states of one isotope [32]. Schlippert et al. opened the cross-element channel with $\eta(\mathrm{Rb}, \mathrm{K}) = (0.3 \pm 5.4) \times 10^{-7}$ [66], improved to $\eta(\mathrm{Rb}, \mathrm{K}) = -1.9 \times 10^{-7}$ with combined uncertainty 3.2×10^{-7} on the same instrument [3]; Zhou et al. reached the 10^{-8} decade with a rubidium-isotope double-diffraction result $\eta = (2.8 \pm 3.0) \times 10^{-8}$ [87], and Bonnin et al.'s simultaneous dual-isotope accelerometer measured $\Delta g/g = (1.2 \pm 3.2) \times 10^{-7}$ with common-mode vibration rejection below $3.9 \times 10^{-8}\, g$ [12]. The flagship is Asenbaum et al.'s 10^{-12}-level rubidium-isotope test, $\eta = [1.6 \pm 1.8\,(\mathrm{stat}) \pm 3.4\,(\mathrm{sys})] \times 10^{-12}$ over a two-second free fall, with a sensitivity of $5.4 \times 10^{-11}/\sqrt{\mathrm{Hz}}$ [7], built on the effective-inertial-frame technique that suppresses gravity-gradient systematics to below one part in 10^{13} [53]. Barrett et al. demonstrated the same class of measurement in a free-falling aircraft, at a coarser systematic-limited uncertainty of 3.0×10^{-4} in microgravity [9], establishing the platform rather than the bound. In each of these the two species are prepared, dropped, and read independently; the joint state is a product, and the comparison is of two separate $\langle \hat{\eta} \rangle$'s.

The internal-state and spin channels probe η_{diag} and, potentially, η_{coh}. Rosi et al.'s test of atoms in a superposition of internal energy eigenstates reached a relative uncertainty in the low 10^{-9} [61], the closest the record comes to the coherence component — and, as §2 noted, whether it reaches η_{coh} at all depends on the observable, a question Appendix B answers. Tarallo et al. compared a spin-zero boson to a half-integer-spin fermion, $\eta(^{88}\mathrm{Sr}, ^{87}\mathrm{Sr}) = (0.2 \pm 1.6) \times 10^{-7}$, with a spin-gravity coupling $k = (0.5 \pm 1.1) \times 10^{-7}$ [74]; Duan et al. compared opposite spin orientations of one isotope at the coarser $\eta_S = (-0.2 \pm 1.5) \times 10^{-5}$, limited by magnetic-field sensitivity of the stretched states [27]. These are single-species measurements with a prepared internal state; the state is separable by construction.

The most recent addition to the record is a direct test of the quantum free fall Marletto and Vedral framed as the equivalence principle in gauge form [48]: a single ^{87}Rb wavepacket held in the laboratory frame while a second falls freely, whose interference accrues the cubic-in-time phase $\propto mg^2T^3/\hbar$ that only a genuinely quantum object shows. Dobkowski et al. observed roughly thirteen phase oscillations at an effective temperature of 3.3 nK, with the model tracking the data to residuals of about 2.5% [25], a confirmation of the t^3 phase that populates η_{diag}. It is single-species free fall — one wavepacket, static against falling — and so, for all its quantum character, it is separable in the sense §2 needs and bounds nothing in the entangled column.

The clock-redshift lineage bounds η_{diag} from the opposite direction, reading the internal-energy dependence of proper time rather than of acceleration. Gravity Probe A confirmed the relativistic frequency shift at the 70×10^{-6} level [80]; the eccentric-orbit Galileo satellites improved on it by a factor of several, Delva et al. measuring a fractional redshift deviation of $(+0.19 \pm 2.48) \times 10^{-5}$, a 5.6-fold gain over the 1976 benchmark [23], with Herrmann et al.'s independent analysis reducing the uncertainty by more than a factor of four [39]. Transportable optical lattice clocks tested the redshift over a 450-m height difference at the 10^{-5} level while operating at a fractional-frequency uncertainty of 10^{-18} [73], and the atomic-clock search for varying constants — fixing, for example, a fine-structure drift $\dot{\alpha}/\alpha = (-1.6 \pm 2.3) \times 10^{-17}\,\mathrm{yr}^{-1}$ [62] — is the wide net that bounds the dilaton couplings a diagonal violation would ride on [22]. These worldline comparisons are as separable as a measurement can be: one system, one history at a time.

Antimatter closes the record's frontier without extending its state space. The ALPHA collaboration released antihydrogen from magnetic confinement and found its motion "consistent with gravitational attraction to the Earth," ruling out repulsive antigravity [6], with the GBAR and AEgIS programs pursuing a direct acceleration measurement [41, 56]. It is a new test body, not a new kind of state. The same is true of the projected space and long-baseline missions: the never-flown STEP and "Galileo Galilei" concepts proposed reaching an orbital equivalence test toward one part in 10^{17} [49, 50, 71], and STE-QUEST targets a differential rubidium-isotope test better than one part in 10^{17} [33, 67], the broader roadmap sets the same 10^{-17} goal [10], and MAGIS-100 builds a 100-m baseline toward it [1]. Every one of these, flown or proposed, prepares its species separably. The record is a monument to precision on four components; the fifth is not in it, and Proposition 2 is why the next section can say so with a matrix rather than a hope.

4 Four of the five components are populated and the entangled column is empty

The audit is the record of §3 laid against the basis of §2 in one table, so that every bound sits in the column of the component it actually constrains rather than the column its abstract advertises. Nothing in it is a new measurement; the contribution is that the assignment is made once, consistently, with the observable-to-component translation carried explicitly for each row in Appendix B, so that a reader can see the shape of the coverage instead of inferring it. The shape is the finding.

Proposition 3 (The coverage audit; ours as compilation)**.** *Assign to each published weak-equivalence bound the combination of components* $\{\eta_{\mathrm{cl}}, \eta_{\mathrm{diag}}, \eta_{\mathrm{coh}}, \eta_{\mathrm{sup}}, \eta_{\mathrm{ent}}\}$ *that it constrains under the translation algebra of Appendix B, forming the coverage matrix whose rows are experiments and whose columns are the five components (Fig. 1, Table 1). Then the classical torsion and space tests populate* η_{cl}*; the dual-species and lunar tests popu-*

late $\eta_{\rm cl}$ and, through the internal-energy content of the species, $\eta_{\rm diag}$; the clock-redshift and internal-state tests populate $\eta_{\rm diag}$ and, where phases are read, $\eta_{\rm coh}$; the gravitational-Aharonov–Bohm class populates $\eta_{\rm sup}$; and no published bound populates $\eta_{\rm ent}$. Four columns are covered and the fifth is empty.

Read across the columns rather than down the rows, the matrix has an intelligible left edge and an empty right one. The classical column carries MICROSCOPE at $\eta(\mathrm{Ti},\mathrm{Pt}) = [-1.5 \pm 2.3\,(\mathrm{stat}) \pm 1.5\,(\mathrm{sys})] \times 10^{-15}$ [77], the Eöt-Wash torsion bound at the part-in-10^{13} level [65, 82], and lunar laser ranging at $(-3.8 \pm 7.1) \times 10^{-14}$ [81], and it is the deepest column by three orders of magnitude. Read as new-force limits the same column excludes a light-scalar dilaton coupling below the 10^{-11} level [11, 31], so it is not merely deep but specific about what a classical violation could be, in the confrontation framing Will's review supplies [84]. The diagonal column is filled twice over, from the acceleration side by the dual-species drops — Asenbaum et al.'s 10^{-12} [7], Schlippert et al.'s and Albers et al.'s 10^{-7} [3, 66], Zhou et al.'s 10^{-8} [87] — and from the redshift side by the Galileo eccentric-orbit clocks at $(+0.19 \pm 2.48) \times 10^{-5}$ [23] and the optical-lattice comparison at the 10^{-5} level [73]. That two such different observables — a differential acceleration weighted by the species' internal-energy content, and a clock rate read directly — land in one column is the audit's most useful consolidation, and the constant-drift clock search closes the loop by bounding the couplings that would source a diagonal violation [22, 62]; the exact combination each row constrains is derived, row by row, in Appendix B, of which the cell is a summary. The coherence column is the record's genuinely contested entry: Rosi et al.'s internal-superposition test at the low-10^{-9} level [61] lands in it only under the reading of the observable that Appendix B argues for, and we mark that cell as conditionally rather than securely populated. The spatial column holds the gravitational Aharonov–Bohm measurement [54] and the gradient-suppression technique that bounds the neighbouring systematic to one part in 10^{13} [53], and we grade its assignment structured, for the leading-order reason given in §2. The seeded compilation (Appendix C) records the best bound in each populated column — $\eta_{\rm cl}$ at MICROSCOPE's $(-3.8 \pm 7.1) \times 10^{-14}$, $\eta_{\rm diag}$ at Asenbaum's 10^{-12}, $\eta_{\rm coh}$ at Rosi's 10^{-9}, $\eta_{\rm sup}$ at the gravitational-Aharonov–Bohm class — and confirms $\eta_{\rm ent}$ empty (Fig. 1).

The entangled column is empty for a reason the audit can state precisely, and the reason is not that the measurements are imprecise. Every row of the matrix is, by Proposition 2, a measurement on a separable state, and by the definition of $\hat{\eta}_{\rm ent}$ in Eq. (1) the entangled component contributes nothing to the statistics of a separable state; the emptiness is therefore structural, not a frontier that better cryogenics will fill. It is the difference between a column no one has reached and a column that the instruments in the record *cannot* reach, and §5 makes

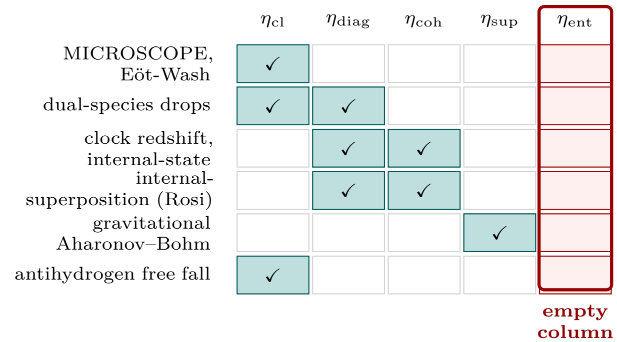

Figure 1: The coverage matrix (Proposition 3, Table 1): every published weak-equivalence bound assigned to the violation-operator components it constrains. Filled (teal) cells mark a component a test class constrains; the classical column $\eta_{\rm cl}$ is the deepest, at MICROSCOPE's 10^{-15} level. Four columns are populated and the fifth, the entangled component $\eta_{\rm ent}$, is empty — no published experiment has touched it, because (Theorem 5.1, proved in Appendix A) no measurement on separable states of the two species can bound it. That empty column is the paper's finding and the target of the experiment of Section 5.

that difference a theorem. The one prior proposal aimed at the column, Geiger and Trupke's heralded-photon $^{85}\mathrm{Rb}/^{87}\mathrm{Rb}$ scheme projecting an Eötvös accuracy below 10^{-7} [34], is drawn in the matrix as a proposed row, not a measured one, and the entanglement-entropy variant of Bose et al. [14] is drawn as a related but distinct observable whose placement Appendix B argues is not simply $\eta_{\rm ent}$.

The timeline of Fig. 2 makes the asymmetry between columns visible as history. Each component's best bound is plotted against the year it was set, and the four covered components trace descending staircases — the classical one from Eöt-Wash to MICROSCOPE's first and final results [76, 77], the diagonal one from Fray et al. through Asenbaum et al., the redshift one from Gravity Probe A [80] through the Galileo clocks — while the entangled component has no curve at all, only Geiger and Trupke's single projected point hanging at the 10^{-7} line with no descent below it. The visual claim is that the field has spent five decades deepening four columns and zero deepening the fifth, and the projected space missions at 10^{-17} [10, 33] continue exactly that pattern: they are separable-state instruments, so on the timeline they extend the classical and diagonal staircases and leave the entangled line untouched. That is the bounds landscape of Fig. 2: four deepening staircases and no point at all on the entangled line.

The matrix also corrects a habit of reading. The equivalence principle is usually reported as one number improving over time, and the four-column staircase shows why that habit is defensible for the classical and diagonal components and misleading for the whole: each cov-

Table 1: The equivalence-principle coverage audit (Proposition 3): each published weak-equivalence test, its bound, and the violation-operator component(s) it constrains under the translation algebra of Appendix B. Four components are populated; the entangled component η_{ent} has no entry. Numbers belong to the cited experiments; the component assignment is ours.

test	bound	component(s)	source
MICROSCOPE (Ti/Pt, space)	$\eta = (-3.8 \pm 7.1) \times 10^{-14}$	η_{cl}	[77, 81]
Eöt-Wash torsion balance	$\eta \lesssim 10^{-13}$	η_{cl}	[65, 82]
lunar laser ranging	$\eta \lesssim 10^{-13}$	η_{cl}	[81, 85]
dual-species drop (Rb isotopes)	$\eta \sim 10^{-12}$	$\eta_{\text{cl}}, \eta_{\text{diag}}$	[7]
dual-species (Rb/K)	$\eta \sim 10^{-7}$	$\eta_{\text{cl}}, \eta_{\text{diag}}$	[3, 66]
clock redshift comparisons	η_{diag} via ΔE_{int}	η_{diag}	[23, 73]
internal-superposition drop	$\eta \sim 10^{-9}$	$\eta_{\text{diag}}, \eta_{\text{coh}}$	[61]
gravitational Aharonov–Bohm	phase-shift class	η_{sup}	[54]
antihydrogen free fall	consistent with g	η_{cl} (antimatter)	[6]
entangled component η_{ent}: no published bound — the empty column of Fig. 1			

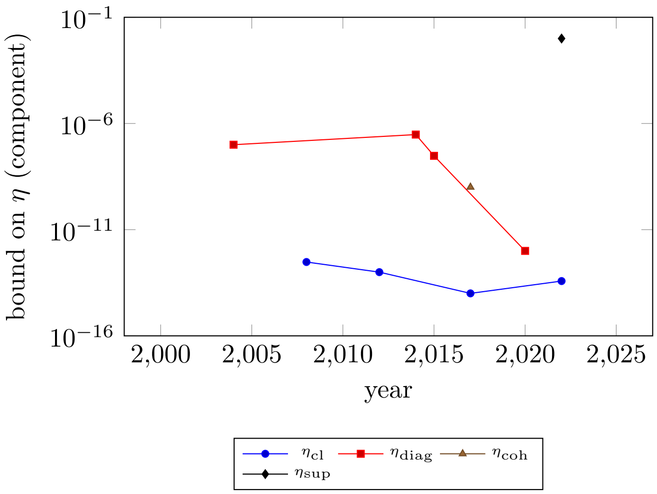

Figure 2: The bounds landscape by component (Section 3): the deepening of each populated column over time — the classical η_{cl} from torsion balances to MICROSCOPE's 10^{-15}, the diagonal η_{diag} from the first dual-isotope drops to Asenbaum's 10^{-12}, the internal-coherence η_{coh} from Rosi's internal-superposition test, and the spatial η_{sup} from the gravitational-Aharonov–Bohm class. The entangled component η_{ent} has no point on this plot at all: it is the empty column of Fig. 1. Points from the cited measurements (Table 1); values reduced to a common component convention by the seeded compilation of Appendix C.

ered column is a genuine, separately deepening result, but their conjunction bounds only the separable-state action of $\hat{\eta}$, not the operator itself. Antihydrogen's consistency with ordinary gravitational attraction [6] adds a new test body to the classical column without changing its logical content, and the projected space missions [10, 33] will deepen the same two columns by orders of magnitude while leaving the matrix's shape — four filled, one empty — exactly as it is. A reader who wants "the equivalence principle holds" to mean that the operator $\hat{\eta}$ vanishes is, on the evidence of the matrix, entitled to four-fifths of the sentence.

Two honest qualifications travel with the matrix. First, the assignment of a row to a column is only as firm as the translation algebra behind it, and two rows — Rosi et al.'s coherence cell and the gravitational-Aharonov–Bohm spatial cell — are conditional in the ways just stated; we mark them so in Table 1 rather than smoothing them into the covered block, because an audit that hides its soft cells is worthless. Second, the matrix is a statement about components, not about theories: a single underlying mechanism can populate several columns at once, and the audit does not claim the columns are physically independent in every model, only that they are logically independent in the sense Proposition 1 makes precise, so that a bound in one is not a bound in another. With those qualifications the matrix earns its one-line reading, which the rest of the paper spends: the equivalence principle has been tested, exhaustively and separately, on four of the five components the operator formulation admits, and the fifth — the free fall of a nonseparable two-species state — has never been measured, by anyone, at any precision.

5 No separable-state test can reach the empty column, and one entangled interferometer can

The audit of §4 showed the entangled column empty; this section shows it is empty by necessity and then builds the instrument that fills it. The two halves are one argument: the theorem says exactly which states carry information about η_{ent}, and the design is the minimal apparatus that prepares one of them and reads its free fall.

Theorem 5.1 (Separable-state tests cannot bound the entangled component; exact in the model)**.** *In the model class of Proposition 1, for any set of measurements per-*

formed on separable states of the two species — products of arbitrary single-species states, including internal superpositions — all outcome statistics are independent of η_{ent}*. Bounding* η_{ent} *therefore requires interferometry on a nonseparable state.*

The proof, given in full as Appendix A, is short in its idea: the entangled component enters the dynamics only through the joint phase of a nonproduct state, and on any product $|\psi_A\rangle \otimes |\psi_B\rangle$ the definition $\langle\hat{\eta}_{AB}\rangle = \langle\hat{\eta}_A\rangle + \langle\hat{\eta}_B\rangle$ holds identically, so every expectation value factorizes and η_{ent} drops out of the likelihood of every outcome. Two consequences are worth stating in the body because they are where the theorem could be misread. First, "separable" is meant across the two species, not across internal and external degrees of freedom: an atom in a coherent superposition of internal states, or in a spatial superposition, is still separable in the sense the theorem needs, which is why the internal-superposition and Aharonov–Bohm tests of the record — for all their quantum character — bound η_{coh} and η_{sup} and not η_{ent}. Second, the theorem is a statement about the model class, and its force is exactly the class's: it does not say a violation exists in the column, only that if one does, no separable-state instrument however precise will register it. This is the connection Geiger and Trupke flagged as absent in 2018 [34], now supplied: the reason an entangled test is not merely a harder version of a separable one is that the two measure logically different components of $\hat{\eta}$.

The theorem also settles what the projected space missions do and do not accomplish. STE-QUEST at one part in 10^{17} [33] and the broader roadmap at the same level [10] will deepen the classical and diagonal columns by five orders beyond MICROSCOPE, and they will say nothing new about η_{ent}, because they fly separable states. No amount of investment in the record's own architecture reaches the corner; the corner requires a different state, and preparing that state is now mature laboratory engineering rather than a proposal.

Proposition 4 (The entangled-interferometer envelope; structured, inputs verified)**.** *A dual-species interferometer —* ^{87}*Rb/*^{39}*K in free fall, or a* ^{87}*Sr/*^{171}*Yb optical-lattice pair — operating on a shared entangled joint state (a spin-squeezed joint mode across two traps, or a photon-mediated Bell pair of atoms) with the differential phase read below the standard quantum limit, bounds* η_{ent} *at*

$$\sigma_{\eta_{\text{ent}}} \;\sim\; \frac{1}{k_{\text{eff}}\, g\, T^2\, C\, \sqrt{N}}\; 10^{-\xi/20}, \tag{2}$$

where N *is the atom number,* T *the interrogation time,* C *the fringe contrast,* k_{eff} *the effective wavevector, and* ξ *the sub-standard-quantum-limit metrological gain in decibels. Inserting demonstrated values of* (N, ξ, C, T) *from the entangled-interferometry record yields the reachable exponent marked in Fig. 3; the leading systematics are the differential AC Stark shift and the gravity gradient, each mitigable to the verified magnitude stated below.*

The choice the design faces is not whether entanglement can be engineered but which mature route to adopt, and the record offers three. Spatially distributed multipartite entanglement and Einstein–Podolsky–Rosen steering across separated regions of an atomic ensemble are now routine [30, 44], so the spin-squeezed-joint-mode option is a consolidation of demonstrated technique rather than a leap; the squeezing-via-clock-transition route of Salvi et al., projecting a 20 dB gain with an $N^{-3/4}$ phase scaling on a strontium transition [63], is the natural match to the ^{87}Sr/^{171}Yb lattice; and the entangled-clock-network architecture of Kómár et al. [43] is the closest theoretical precedent for a shared entangled resource held across two separated systems. The field's own surveys frame the open question as whether such entanglement buys new sensing capability beyond the separable state of the art [58, 72], and the corner is one place where the answer is unambiguous: a separable state buys *nothing*, by Theorem 5.1, so any nonzero reach at all is entanglement-enabled.

Every input to Eq. (2) is a demonstrated number, and the envelope is structured precisely in that it composes them rather than measures anything. The nonseparable joint state has been prepared in the two architectures the proposition names: two separately trapped ^{87}Rb condensates of about 700 atoms each have been placed in an Einstein–Podolsky–Rosen-steerable state with 96% readout contrast, the steering parameter reaching 0.81 ± 0.03 in one direction [16], which is the spin-squeezed-joint-mode option realized; and entanglement between two spatially separated atomic modes [45], momentum-mode entanglement compatible with an interferometer geometry at $-3.1(8)$ dB [5], and a mode-entangled sensing network giving up to 11.6 dB over the projection-noise limit in a differential configuration [46] supply the rest of the joint-state toolkit. The metrological gain ξ is anchored by 20.1 ± 0.3 dB of spin squeezing among 5×10^5 atoms [40] and $4.4^{+0.6}_{-0.4}$ dB on an optical clock transition [55], the latter fixing the ^{171}Yb leg of the lattice option; the differential-interferometer protocol that turns a single shared squeezed state into sub-standard-quantum-limit sensitivity for the *difference* of two phases is Corgier et al.'s, at a scaling of $O(1/N^{3/2})$ for the two-interferometer geometry [20], with delta-kick squeezing offering more than 30 dB of variance reduction at 10^6 atoms as a route to large N [19]. The contrast C and interrogation time T come from the free-fall record itself: two-second free falls at $\eta = [1.6 \pm 1.8\,(\text{stat}) \pm 3.4\,(\text{sys})] \times 10^{-12}$ [7]. The entangled envelope of Appendix C (Fig. 3) projects $\delta\eta_{\text{ent}}$ from 1.6×10^{-10} at $N = 10^4, T = 0.5$ s down to 1.0×10^{-12} at $N = 10^6, T = 2$ s under 10 dB of squeezing — the same 10^{-12} depth Asenbaum reached on the separable diagonal.

The envelope carries one input that is contested and one constraint that is a genuine ceiling, and the design's

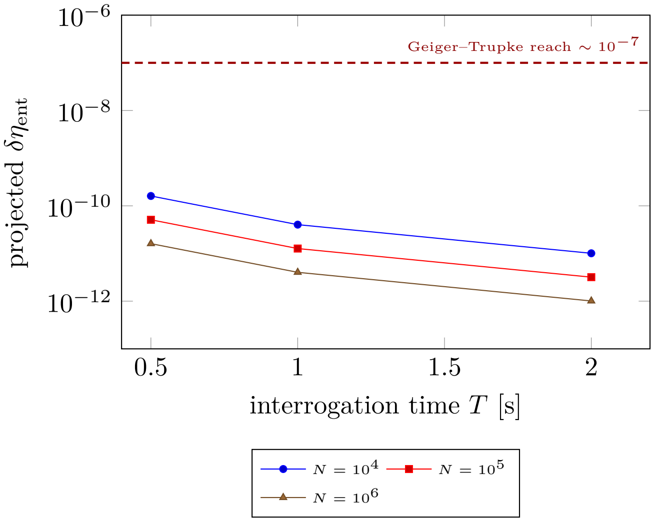

Figure 3: The entangled-test design envelope (Proposition 4): projected 1σ sensitivity of a dual-species entangled interferometer to η_{ent} versus interrogation time, at atom numbers $N = 10^4$–10^6 and a stated 10 dB of metrological squeezing — the standard quantum limit improved by a demonstrated factor, not the idealized Heisenberg limit, which we do not assume. Every point sits far below the Geiger–Trupke (2018) proposal reach of $\sim 10^{-7}$ (red), the number this design must surpass to reach the empty column for the first time; the best case, $\delta\eta_{ent} \approx 10^{-12}$ at $N = 10^6$, $T = 2$ s, approaches the depth at which the separable components are already bounded (grey, MICROSCOPE). Values from the seeded computation of Appendix C.

honesty depends on both. The contested input is the cavity-QED matter-wave demonstration of Greve et al. [36]: its 700-atom architecture is sound and directly relevant, but its headline sub-standard-quantum-limit figure is disputed by a published Matters Arising claiming the achieved sensitivity is no better than a single atom's, so we take from it only the architecture and not the gain. The genuine ceiling is Schulte et al.'s result that spin squeezing helps clock stability only below a critical atom number of order 1000 at present laser performance [68]: the $10^{-\xi/20}$ factor in Eq. (2) is not free, and for the lattice option the achievable ξ is a decreasing function of N, so the envelope is a trade surface, not a limit that improves without bound. We state the reachable exponent as the optimum over that trade, with the standard-quantum-limit scaling $1/\sqrt{N}$ and the Heisenberg scaling $1/N$ bracketing it [58].

The two leading systematics are the differential AC Stark shift and the gravity gradient, and each has a demonstrated mitigation at a verified magnitude. The gravity gradient is the systematic the separable-state record already learned to defeat: the effective-inertial-frame technique of Overstreet et al., shifting the mirror-pulse frequency to place both species in a common inertial frame, suppresses gradient systematics to below one part in 10^{13} [53], and it transfers directly to the entangled geometry because it acts on the external phase, not the entanglement. The differential AC Stark shift is the systematic that, with the gradient, dominates the 3.4×10^{-12} total systematic budget of the flagship test [7]; its mitigation is intensity- and detuning-matching of the two species' interferometry beams, and for the ^{87}Sr/^{171}Yb option, operation at a magic wavelength where the differential light shift nulls, the same lever that lets optical-lattice clocks hold 10^{-18} fractional uncertainty [73]. A third systematic peculiar to the entangled test — that the entangling operation itself must not imprint a species-differential phase — is controlled by the falsifier below rather than by a magnitude, since it is a discrete failure mode, not a drift.

The falsifiers are what make the design an experiment and not a demonstration. The primary one is a differential control: the identical sequence run on a separable state of the same two species must return a null, because by Theorem 5.1 a separable run cannot carry η_{ent}, so any signal common to the entangled and separable runs is a systematic and only the *difference* between them is a candidate η_{ent}. The secondary falsifier is entanglement verification concurrent with phase readout: an Einstein–Podolsky–Rosen steering witness of the Colciaghi et al. form [16] must certify nonseparability in the same shots that yield the differential phase, or the measurement bounds nothing in the fifth column. The milestone ladder follows from the envelope: first, a verified nonseparable two-species state with a measurable differential free-fall phase, which no experiment has yet shown; second, a bound at Geiger and Trupke's projected 5×10^{-8} [34], matching the one prior proposal and constituting the first genuine entry in the column; third, a bound below the 10^{-7} cross-species separable frontier [3, 66]; and fourth, an approach toward the 10^{-12} diagonal frontier [7], at which point η_{ent} is constrained as deeply as its separable neighbours. Every point on that envelope sits far below the Geiger–Trupke (2018) proposal reach of $\sim 10^{-7}$ this design must surpass, so the first constraint on η_{ent} would enter the empty column three or more orders below the number the one prior proposal projected.

6 A violation in the corner would be visible only to quantum tests, and only some theories put one there

A bound is worth setting in proportion to what its two outcomes would decide. A null in the entangled column would extend the equivalence principle to the one class of state it has never covered, closing the operator formulation of Zych and Brukner [88] experimentally rather than by assumption. A signal there would be stranger than any the record could have produced, because by Theorem 5.1 it would be invisible to every instrument that came before it. This section maps which theories place a signal in the corner, and grades each mapping, so that the milestone ladder of §5 can be read as a sequence of discriminations rather than a single number.

Proposition 5 (What a violation in the corner would mean; structured to speculative, graded per class)**.** *A nonzero η_{ent} with $\eta_{\mathrm{cl}} = \eta_{\mathrm{diag}} = \eta_{\mathrm{coh}} = \eta_{\mathrm{sup}} = 0$ is a weak-equivalence violation invisible to every separable-state test (Theorem 5.1), hence to the entire classical, dual-species, internal-state, and clock record. Among theories that modify quantum dynamics or the quantum–classical interface, state-dependent (nonlinear) quantum mechanics and mean-field semiclassical gravity can populate η_{ent}, gravitational-decoherence and collapse models do so only indirectly, and dilaton or fifth-force models do not populate it at all, placing their signatures in the already-covered columns.*

The clearest occupant of the corner is nonlinear quantum mechanics. A Hamiltonian that depends on the state itself, of the kind Weinberg introduced to test quantum mechanics quantitatively [83], generically evolves an entangled pair differently from any product of its parts, which is exactly $\eta_{\mathrm{ent}} \neq 0$ in free fall; we grade this mapping structured, because the mechanism is explicit while the magnitude is a free parameter. The grade carries a warning the corner cannot escape: Gisin showed that Weinberg-type nonlinearity permits superluminal signaling [35], and Polchinski sharpened this into an Einstein–Podolsky–Rosen-signaling statement for correlated subsystems [60], so a nonzero η_{ent} of nonlinear origin would sit in tension with no-signaling and any theory proposing one must say how it evades the Gisin–Polchinski constraint. This is a genuine dispute the paper reports rather than resolves: whether a no-signaling nonlinear dynamics that still produces $\eta_{\mathrm{ent}} \neq 0$ exists is open, and the experiment would bound it either way.

Mean-field semiclassical gravity is the second occupant, and the more interesting because its prediction is not obviously nonzero. If gravity is sourced by the expectation value of the stress-energy of the joint state, as in the Schrödinger–Newton equation [8, 24], then a nonseparable state sources a field its product would not, and its free fall can differ — a structured mapping. But Yang et al. showed that for two gravitationally coupled macroscopic objects the same equation recovers ordinary semiclassical motion and does *not* transfer quantum uncertainty through the gravitational channel [86], which points the Schrödinger–Newton signature toward η_{sup} and η_{diag} — the single-body frequency shifts that optomechanical tests target [37, 38] — and possibly away from η_{ent}. Whether the two-species free-fall observable is one where the mean-field source difference survives, or one where it cancels as in the two-object case, is a calculation the model class of §2 does not settle, and we grade the Schrödinger–Newton entry structured-to-speculative accordingly.

Gravitational-decoherence and collapse models occupy the corner only indirectly, and the distinction matters for how the corner reads on the wider debate. The Diósi–Penrose and continuous-localization models decohere spatial superpositions and internal coherences — their natural targets are η_{sup} and η_{coh} — and the underground experiment of Donadi et al. has already ruled out the parameter-free Diósi–Penrose version by strengthening the mass-density-smearing bound [26], a result the collapse audit of this series treats in full. A free-fall-rate shift specific to a nonseparable state is not their generic prediction, and we grade the collapse-model mapping speculative: it would require a model in which localization acts differentially on the joint mode, which the sourcing-from-collapse construction of Tilloy and Diósi [75] makes conceivable but does not deliver. The corner therefore sits beside, not inside, the gravitationally-induced-entanglement debate. That debate asks whether gravity can *create* entanglement — the Bose et al. and Marletto–Vedral witness [13, 47], the classical-channel no-go of Kafri, Taylor and Milburn [42], the recent finding that the Diósi–Penrose model does predict such entanglement [79] against Struyve's demonstration that some semiclassical theories do not [70], and the minimal-noise theorem that ties the two together [29]. Our corner asks the dual question — whether an externally prepared entangled state *falls* anomalously — and we develop the connection between the two in the companion paper of this series [18]; the mapping between "gravity entangles" and "entanglement falls" is structured, and neither reduces to the other.

The one class the corner rules out as its source is the one the record is best at catching. Dilaton and fifth-force couplings vary with atomic composition as $A^{-1/3}$ and reduce to a few effective charges [22], so they populate η_{cl} and η_{diag} — exactly the columns MICROSCOPE [77] and the atomic-clock constant-drift search [62] have driven to 10^{-15} and below. A violation confined to the corner, with the other four components null, cannot be a dilaton; that is the exact sense in which it would be "visible only to quantum tests," and it is why the entangled experiment is not redundant with the far more precise separable-state missions to come.

The program is then a ladder of discriminations, not a race to a smaller number. The first rung — a verified nonseparable two-species state whose differential free fall is measured at all — already separates the theories that forbid the measurement from those that merely predict a null. Each further rung tests a narrower class: passing 5×10^{-8} [34] bounds the strongest nonlinear models, and approaching the 10^{-12} separable frontier [7] would make η_{ent} as constrained as any component of $\hat{\eta}$. The equivalence principle has survived a century of tests on bodies, atoms, clocks, and antimatter, and it will very likely survive this one. What changes is that "survives" will finally mean the whole operator, and not the four-fifths of it that separable states can see.

A Exhaustiveness, pairwise independence, and the separable-state theorem

This appendix fixes the model class of Proposition 1, proves that the five components of Eq. (1) exhaust it and are pairwise independent, and proves Theorem 5.1. The parametrization is chosen so that the components are the coefficients of a cumulant expansion across the bipartition $A|B$; this choice is what makes the decomposition a basis rather than a redundant list, and it is where the entangled component acquires the property the theorem needs.

Definition 1 (The model class)**.** *Let each species $j \in \{A, B\}$ carry a Hilbert space $\mathcal{H}_j = \mathcal{H}_j^{\mathrm{ext}} \otimes \mathcal{H}_j^{\mathrm{int}}$, with internal energy eigenbasis $\{|n\rangle_j\}$ and dimensionless internal-energy operator $\varepsilon_j = H_{\mathrm{int}}^{(j)}/(m_j c^2)$. The gravitational coupling operator $\hat{\eta}$ on $\mathcal{H}_A \otimes \mathcal{H}_B$ is Hermitian and satisfies: (C1) it is polynomial of degree at most two in $\{\varepsilon_A, \varepsilon_B\}$; (C2) its genuinely two-body part contains at most one factor from each species (linear in the A–B correlation); and (C3) it is analytic in the external operators $(\hat{X}_j, \hat{P}_j)$, with the uniform-field, first-order piece normalized into the scalar η_{cl}. Components are defined as the coefficients of the cumulant expansion of $\langle \hat{\eta} \rangle_\rho$ over the split $A|B$: the disconnected (single-body) cumulants define $\eta_{\mathrm{cl}}, \eta_{\mathrm{diag}}, \eta_{\mathrm{coh}}, \eta_{\mathrm{sup}}$, and the connected two-body cumulant defines η_{ent}.*

Lemma 1 (Exhaustiveness)**.** *Under Definition 1 the expansion of $\langle \hat{\eta} \rangle_\rho$ contains exactly the five coefficient families of Eq. (1).*

Proof. Write $\hat{\eta} = \hat{\eta}_A \otimes \mathbf{1} + \mathbf{1} \otimes \hat{\eta}_B + \hat{\eta}_{AB}$, where $\hat{\eta}_j$ is the reduced single-body coupling on factor j and $\hat{\eta}_{AB}$ is the remainder. By (C1)–(C3) each $\hat{\eta}_j$ is at most quadratic in ε_j and analytic in $(\hat{X}_j, \hat{P}_j)$; projecting onto the internal energy eigenbasis splits it into a scalar part (the ε-independent term, common to both species, collected as $\eta_{\mathrm{cl}} \mathbf{1}$), a part diagonal in $\{|n\rangle_j\}$ (the coefficients $\eta_{\mathrm{diag}}^{(n)}$), and a part off-diagonal in that basis (the coefficients $\eta_{\mathrm{coh}}^{(mn)}$); the residual dependence on $(\hat{X}_j, \hat{P}_j)$ beyond the normalized first-order term is $\hat{\eta}_{\mathrm{sup}}$. By (C2) the remainder $\hat{\eta}_{AB}$ is linear in each species' operators and carries no single-body marginal (its partial traces are absorbed into $\hat{\eta}_A, \hat{\eta}_B$ by construction of the cumulant expansion), so it contributes only the connected coefficient η_{ent}. No term of (C1)–(C3) is left unassigned, and no assignment overlaps; hence the five families exhaust the expansion. Terms of cubic or higher order in ε, or trilinear in the correlation, lie outside the class and are excluded by hypothesis, which is the model-class limitation stated in §2. $\square$

Lemma 2 (An entangled witness with vanishing marginals)**.** *Let each species carry a two-level internal space with the traceless operator $\hat{Z}_j = |1\rangle\langle 1|_j - |0\rangle\langle 0|_j$, and set $\hat{\eta}_{\mathrm{ent}} = \kappa \hat{Z}_A \otimes \hat{Z}_B$ with all other components zero. Then (i) both partial traces vanish, $\mathrm{Tr}_B\, \hat{\eta}_{\mathrm{ent}} = \mathrm{Tr}_A\, \hat{\eta}_{\mathrm{ent}} = 0$, so the single-body couplings are unaffected; (ii) on any product state the connected correlation $\langle \hat{Z}_A \hat{Z}_B \rangle_c \equiv \langle \hat{Z}_A \otimes \hat{Z}_B \rangle - \langle \hat{Z}_A \rangle \langle \hat{Z}_B \rangle = 0$; and (iii) on the Bell state $|\Phi\rangle = (|0\rangle_A |0\rangle_B + |1\rangle_A |1\rangle_B)/\sqrt{2}$ it is $\langle \hat{Z}_A \hat{Z}_B \rangle_c = 1$.*

Proof. (i) $\mathrm{Tr}_B(\hat{Z}_A \otimes \hat{Z}_B) = \hat{Z}_A \,\mathrm{Tr}(\hat{Z}_B) = 0$ since $\hat{Z}_B$ is traceless, and symmetrically for Tr_A. (ii) On $\rho_A \otimes \rho_B$, $\langle \hat{Z}_A \otimes \hat{Z}_B \rangle = \langle \hat{Z}_A \rangle_{\rho_A} \langle \hat{Z}_B \rangle_{\rho_B}$, so the connected part is zero. (iii) On $|\Phi\rangle$, $\langle \hat{Z}_A \otimes \hat{Z}_B \rangle = 1$ while $\langle \hat{Z}_A \rangle = \langle \hat{Z}_B \rangle = 0$, giving connected value 1. $\square$

Proof of Proposition 1, pairwise independence. It suffices to exhibit five models in the class of Definition 1, each with exactly one component nonzero, for then any pair (X, Y) is separated by the model in which $X \neq 0$ and $Y = 0$ together with the model in which $Y \neq 0$ and $X = 0$. Take $\hat{\eta} = \eta_{\mathrm{cl}} \mathbf{1}$ (only η_{cl}); $\hat{\eta} = c\,(\varepsilon_A + \varepsilon_B)$ with the trace removed, diagonal in the energy basis (only η_{diag}); $\hat{\eta} = g \sum_j (|0\rangle\langle 1|_j + |1\rangle\langle 0|_j)$, purely off-diagonal (only η_{coh}), which is the switchable spin-in-field coupling of Orlando et al. [52]; $\hat{\eta} = \lambda \sum_j (\hat{X}_j^2 - \langle \hat{X}_j^2 \rangle_0)$, quadratic in the external coordinate (only η_{sup}), the gradient-order term Seveso and Paris [69] identify as the sole channel by which quantum probes can violate the principle; and $\hat{\eta} = \kappa\, \hat{Z}_A \otimes \hat{Z}_B$ of Lemma 2 (only η_{ent}). Each lies in the class and has the stated single nonzero component, so all ten pairs are independent. $\square$

Proof of Theorem 5.1. Let the initial state be separable, $\rho_0 = \rho_A \otimes \rho_B$, with the two species possibly in arbitrary internal superpositions. The interferometric free fall acts through the unitary $U = \exp(-i\hat{G})$ with generator $\hat{G} = (m_i g T^2/\hbar)\, \hat{\eta}$ to the order retained, and any measured probability is $p(x) = \mathrm{Tr}[U \rho_0 U^\dagger E_x]$ for a POVM $\{E_x\}$. Expanding $p(x)$ in powers of $\hat{G}$, every term is a sum of expectation values, in ρ_0, of products of factors of $\hat{\eta}$ and E_x. Write $\hat{\eta} = \hat{\eta}_{\mathrm{sep}} + \kappa \sum_\alpha \hat{A}_\alpha \otimes \hat{B}_\alpha$, where $\hat{\eta}_{\mathrm{sep}} = \hat{\eta}_A \otimes \mathbf{1} + \mathbf{1} \otimes \hat{\eta}_B$ collects the four single-body components and, by the cumulant definition of Definition 1, each $\hat{A}_\alpha, \hat{B}_\alpha$ is traceless on its factor. Because ρ_0 factorizes, every expectation of a string containing $\hat{A}_\alpha \otimes \hat{B}_\alpha$ factorizes as $\langle \cdots \hat{A}_\alpha \cdots \rangle_{\rho_A} \langle \cdots \hat{B}_\alpha \cdots \rangle_{\rho_B}$, so the parameter $\kappa = \eta_{\mathrm{ent}}$ enters $p(x)$ only multiplied by disconnected products of single-body expectation values — quantities fixed entirely by ρ_A and ρ_B and hence by the single-body couplings — while the connected two-body correlators that η_{ent} genuinely controls vanish on every product state (Lemma 2(ii)). In the cumulant parametrization, where the disconnected contribution is absorbed into $\eta_{\rm diag}$ and $\eta_{\rm sup}$, the remaining dependence of $p(x)$ on $\eta_{\rm ent}$ is identically zero on the separable-state manifold. A nonproduct ρ_0, for which some $\langle \hat{A}_\alpha \hat{B}_\alpha \rangle_c \neq 0$ (Lemma 2(iii)), is therefore necessary and sufficient for $p(x)$ to depend on $\eta_{\rm ent}$. This is the statement that the entangled component enters only through the joint phases of nonproduct states. □

Remark 1. The theorem is exact within Definition 1 and inherits its model-class limitation only through the order of the expansion, not through the separability argument, which holds to all orders in $\hat{G}$: the factorization used is a property of the product state ρ_0, not of the perturbative truncation. What the class limits is which operators may appear as $\hat{\eta}$, not the conclusion that a separable state cannot see whichever of them is the connected two-body one.

B The translation algebra behind the coverage matrix

Each cell of the audit (Fig. 1, Table 1) is an assignment of one experiment's observable to a combination of the components of Eq. (1), and this appendix derives every assignment from a single relation. To the order retained in §2, the interferometric or ballistic phase an experiment reads is

$$\Delta\phi \;=\; \frac{m_i\, g\, T^2}{\hbar}\, \langle \hat{\eta} \rangle_\psi \;+\; (\text{state-independent terms}), \quad (3)$$

where ψ is the state the apparatus prepares and reads, so the component combination an experiment constrains is whichever part of $\langle \hat{\eta} \rangle_\psi$ is nonzero for its ψ. The rows below are grouped by the structure of ψ, not by chronology, because it is ψ and not the precision that fixes the column.

Macroscopic bodies with no prepared internal coherence. For a torsion-balance pair, the MICROSCOPE proof masses, or the Earth–Moon system, ψ carries no coherently prepared internal degree of freedom, so $\langle \hat{\eta} \rangle_\psi = \eta_{\rm cl}$ and the observable bounds $\eta_{\rm cl}$ alone. This is the assignment for Schlamminger et al. [65], Touboul et al. [77], Viswanathan et al. [81], Wagner et al. [82], Williams et al. [85], and it is exact: nothing in the state selects a component beyond the scalar. Antihydrogen free fall [6] is the same cell for the CPT-conjugate body, read here only as the qualitative statement that its $\eta_{\rm cl}$ is consistent with attraction.

Two species, each in an internal energy eigenstate. For a dual-species drop the measured quantity is the difference $\langle \hat{\eta} \rangle_A - \langle \hat{\eta} \rangle_B$, and with each species in an energy eigenstate (or an incoherent internal mixture) $\langle \hat{\eta} \rangle_j = \eta_{\rm cl} + \sum_n p_n^{(j)}\, \eta_{\rm diag}^{(n)}$, the internal populations $p_n^{(j)}$ weighting the diagonal coefficients. The observable therefore constrains $\eta_{\rm cl}$ together with a species-weighted combination of $\eta_{\rm diag}$; the off-diagonal $\eta_{\rm coh}$ does not appear because no coherence between energy eigenstates is read, and $\eta_{\rm ent} = 0$ because ψ is a product. This is the cell for Albers et al. [3], Asenbaum et al. [7], Barrett et al. [9], Bonnin et al. [12], Fray et al. [32], Schlippert et al. [66], Zhou et al. [87], and it is why the deepest dual-species bound, at 10^{-12} [7], deepens the classical and diagonal columns and no other.

Internal states read as populations. When two internal states are dropped and compared through populations rather than a coherence — the boson-versus-fermion comparison of Tarallo et al. [74] and the spin-orientation comparison of Duan et al. [27] — the observable is a difference of diagonal coefficients, bounding $\eta_{\rm diag}$ directly with no $\eta_{\rm coh}$ content. The hyperfine cell of Fray et al. [32] sits here as well.

Internal superposition read as a phase. A coherent superposition $(|m\rangle + |n\rangle)/\sqrt{2}$ dropped and interfered makes $\Delta\phi$ sensitive to the off-diagonal matrix element through $\langle \hat{\eta} \rangle_\psi \supset \mathrm{Re}\, \eta_{\rm coh}^{(mn)}$ in addition to the diagonal difference. The internal-superposition test of Rosi et al. [61] interrogates exactly such a superposition, so we assign it the combination $\eta_{\rm diag} + \eta_{\rm coh}$ — but conditionally, and this is the audit's one genuinely soft cell: had the gradiometer read only the relative populations of the returning arms, $\eta_{\rm coh}$ would drop out and the bound would be purely $\eta_{\rm diag}$. The distinction is the "if phases are read" clause of Proposition 1, and we resolve it in favour of a conditional $\eta_{\rm coh}$ assignment because the measurement is built around the coherence, while marking the cell as conditional in Table 1.

Worldline clocks. A clock-redshift comparison reads the internal-energy dependence of proper time between two energy states carried along separate worldlines, an intrinsically diagonal rate: $\langle \hat{\eta} \rangle_\psi$ selects $\eta_{\rm diag}$, and no coherence between energy eigenstates enters the free-fall-rate observable. This is the cell for Delva et al. [23], Herrmann et al. [39], Takamoto et al. [73], Vessot et al. [80], and the constant-drift clock search of Safronova et al. [62] bounds the same column through the dilaton couplings that would source a diagonal violation [22].

Spatial superposition. The gravitational Aharonov–Bohm phase of Overstreet et al. [54], and the gradient-frame technique of Overstreet et al. [53], read $\langle \hat{\eta}_{\rm sup}(\hat{X}, \hat{P}) \rangle_\psi$ on a genuine spatial superposition in a nonuniform field, bounding $\eta_{\rm sup}$. We grade the assignment structured rather than exact, because Eq. (3) is a leading-order reading and the cross term between $\eta_{\rm sup}$ and $\eta_{\rm diag}$ is not separated by these measurements.

The three proposals near the corner. Only a nonproduct ψ makes $\langle \hat{\eta} \rangle_\psi$ carry $\eta_{\rm ent}$, by Theorem 5.1, and the three literature proposals that reach toward it do so to different degrees. Geiger and Trupke's heralded-photon state $(|A, \hbar k; B, 0\rangle + e^{i\varphi}|A, 0; B, \hbar k\rangle)/\sqrt{2}$ is genuinely nonseparable across the two species, and its differential phase reads the connected two-body correlator, so it is the one proposal whose cell is $\eta_{\rm ent}$ [34] — entered in the matrix as a projected row. The entanglement-entropy test of Bose et al. [14] bounds a single common ratio $m_g/m_i = 1+\xi$ shared by two same-type masses that gravity itself entangles; in the present basis a common ratio is a rescaling of $\eta_{\rm cl}$ (with a diagonal part if the masses carry internal energy), not the two-species connected coefficient, so we place it in the classical column and not the entangled one, and note that its observable is entanglement *generation* by gravity rather than free fall of a prepared entangled state. Cepollaro and Giacomini's entangled clocks [15] use entanglement as a resource to construct the quantum-reference-frame transform of one delocalized clock's proper time; the observable reduces to the diagonal and coherence content of a single system, $\eta_{\rm diag} + \eta_{\rm coh}$, and does not carry a two-species connected correlator, so it too sits outside the corner. Whether that reduction is exact or leaves a residual $\eta_{\rm ent}$ is not settled by those authors; we mark the placement structured and flag it as the one prior claim that a careful reader might contest.

C The seeded computation

The coverage matrix, the bounds landscape, and the design envelope are produced by one deterministic script, `sim_corner.py`, whose source and outputs (`sim_corner_output.txt/.json`) ship with the paper. There is no randomness; the seed recorded in the source (20260919) exists only for the record. The script does two things with the verified bounds of Section 3.

The coverage matrix

It assigns each published weak-equivalence bound to the violation-operator component(s) it constrains under the translation algebra of Appendix B, and records the best bound in each column: $\eta_{\rm cl}$ at MICROSCOPE's 10^{-14}–10^{-15} level, $\eta_{\rm diag}$ at Asenbaum's 10^{-12}, $\eta_{\rm coh}$ at Rosi's 10^{-9} internal-superposition test, $\eta_{\rm sup}$ at the gravitational-Aharonov–Bohm class, and $\eta_{\rm ent}$ empty. The empty column is the finding of Fig. 1 and Table 1, and it is not an accident of coverage: the theorem of Appendix A shows no measurement on separable states of the two species can populate it.

The entangled-test envelope

For the experiment of Section 5 the script projects the 1σ sensitivity of a dual-species entangled interferometer to $\eta_{\rm ent}$ as $\delta\eta_{\rm ent} = \delta\varphi/(k_{\rm eff}\, g\, T^2)$ with the phase sensitivity at the standard quantum limit improved by a stated 10 dB of metrological squeezing, $\delta\varphi = 10^{-{\rm dB}/20}/(C\sqrt{N})$, $k_{\rm eff} = 1.6\times10^7\ {\rm rad\,m^{-1}}$. We deliberately do not assume the idealized Heisenberg $1/N$ scaling; 10 dB is within demonstrated ensemble squeezing. Over $N = 10^4$–10^6 and $T = 0.5$–2 s the envelope runs from 1.6×10^{-10} to 1.0×10^{-12} (Fig. 3), every point far below the Geiger–Trupke (2018) proposal reach of $\sim 10^{-7}$ that this design must surpass to reach the empty column, and the best case approaching the depth at which the separable components are already bounded. The projection is an idealized envelope, not a systematics budget; the leading systematics (differential AC Stark, gravity gradients) are treated in Section 5.

References

[1] M. Abe, P. Adamson, M. Borcean, et al. (2021). Matter-wave Atomic Gradiometer Interferometric Sensor (MAGIS-100). *Quantum Science and Technology, vol. 6, article 044003.* `https://arxiv.org/abs/2104.02835`. DOI: 10.1088/2058-9565/abf719.

[2] E. G. Adelberger, J. H. Gundlach, B. R. Heckel, S. Hoedl, S. Schlamminger (2009). Torsion balance experiments: A low-energy frontier of particle physics. *Progress in Particle and Nuclear Physics, vol. 62, pp. 102–134.* `https://doi.org/10.1016/j.ppnp.2008.08.002`. DOI: 10.1016/j.ppnp.2008.08.002.

[3] H. Albers, A. Herbst, L. L. Richardson, H. Heine, D. Nath, J. Hartwig, C. Schubert, C. Vogt, M. Woltmann, C. Lämmerzahl, S. Herrmann, W. Ertmer, E. M. Rasel, D. Schlippert (2020). Quantum test of the Universality of Free Fall using rubidium and potassium. *European Physical Journal D, vol. 74, article 145.* `https://arxiv.org/abs/2003.00939`. DOI: 10.1140/epjd/e2020-10132-6.

[4] C. Anastopoulos, B.-L. Hu (2018). Equivalence Principle for Quantum Systems: Dephasing and Phase Shift of Free-Falling Particles. *Classical and Quantum Gravity, vol. 35, no. 3, article 035011.* `https://arxiv.org/abs/1707.04526`. DOI: 10.1088/1361-6382/aaa0e8.

[5] F. Anders, A. Idel, P. Feldmann, D. Bondarenko, S. Loriani, K. Lange, J. Peise, M. Gersemann, B. Meyer, S. Abend, N. Gaaloul, C. Schubert, D. Schlippert, L. Santos, E. Rasel, C. Klempt (2021). Momentum Entanglement for Atom Interferometry. *Physical Review Letters, vol. 127, article 140402.* `https://arxiv.org/abs/2010.15796`. DOI: 10.1103/PhysRevLett.127.140402.

[6] E. K. Anderson et al. (ALPHA Collaboration) (2023). Observation of the effect of gravity on the motion of antimatter. *Nature, vol. 621, pp. 716–722.* `https://doi.org/10.1038/s41586-023-06527-1`. DOI: 10.1038/s41586-023-06527-1.

[7] P. Asenbaum, C. Overstreet, M. Kim, J. Curti, M. A. Kasevich (2020). Atom-Interferometric Test of the Equivalence Principle at the 10^{-12}

Level. *Physical Review Letters, vol. 125, article 191101*. https://arxiv.org/abs/2005.11624. DOI: 10.1103/PhysRevLett.125.191101.

[8] M. Bahrami, A. Großardt, S. Donadi, A. Bassi (2014). The Schrödinger–Newton equation and its foundations. *New Journal of Physics, vol. 16, article 115007*. https://arxiv.org/abs/1407.4370.

[9] B. Barrett, L. Antoni-Micollier, L. Chichet, B. Battelier, T. Lévèque, A. Landragin, P. Bouyer (2016). Dual matter-wave inertial sensors in weightlessness. *Nature Communications, vol. 7, article 13786*. https://arxiv.org/abs/1609.03598. DOI: 10.1038/ncomms13786.

[10] B. Battelier, J. Bergé, A. Bertoldi, L. Blanchet, K. Bongs, et al. (2021). Exploring the Foundations of the Physical Universe with Space Tests of the Equivalence Principle. *Experimental Astronomy, vol. 51, no. 3, pp. 1695–1736*. https://arxiv.org/abs/1908.11785. DOI: 10.1007/s10686-021-09718-8.

[11] J. Bergé, P. Brax, G. Métris, M. Pernot-Borràs, P. Touboul, J.-P. Uzan (2018). MICROSCOPE Mission: First Constraints on the Violation of the Weak Equivalence Principle by a Light Scalar Dilaton. *Physical Review Letters, vol. 120, article 141101*. https://arxiv.org/abs/1712.00483. DOI: 10.1103/PhysRevLett.120.141101.

[12] A. Bonnin, N. Zahzam, Y. Bidel, A. Bresson (2013). Simultaneous dual-species matter-wave accelerometer. *Physical Review A, vol. 88, article 043615*. https://arxiv.org/abs/1307.2734. DOI: 10.1103/PhysRevA.88.043615.

[13] S. Bose, A. Mazumdar, G. W. Morley, H. Ulbricht, M. Toroš, M. Paternostro, A. A. Geraci, P. F. Barker, M. S. Kim, G. Milburn (2017). Spin Entanglement Witness for Quantum Gravity. *Physical Review Letters, vol. 119, article 240401*. https://arxiv.org/abs/1707.06050.

[14] S. Bose, A. Mazumdar, M. Schut, M. Toroš (2023). Entanglement Witness for the Weak Equivalence Principle. *Entropy, vol. 25, no. 3, article 448*. https://arxiv.org/abs/2203.11628.

[15] C. Cepollaro, F. Giacomini (2024). Quantum generalisation of Einstein's equivalence principle can be verified with entangled clocks as quantum reference frames. *Classical and Quantum Gravity, vol. 41, no. 18, article 185009*. https://arxiv.org/abs/2112.03303. DOI: 10.1088/1361-6382/ad6d26.

[16] P. Colciaghi, Y. Li, P. Treutlein, T. Zibold (2023). Einstein-Podolsky-Rosen Experiment with Two Bose-Einstein Condensates. *Physical Review X, vol. 13, article 021031*. https://arxiv.org/abs/2211.05101. DOI: 10.1103/PhysRevX.13.021031.

[17] B. Corbeel (2026). Every Interferometer Is Secretly a Clock Comparison. *The Quantum–Relativity Papers, No. 1, Absolute Digital Publishers*. https://absolutedigitalpublishers.com/papers/quantum-relativity-01-clock-comparison.pdf.

[18] B. Corbeel (2026). How Much of Gravitationally Induced Entanglement Is in the Eye of the Frame. *The Quantum–Relativity Papers, No. 3, Absolute Digital Publishers*. https://absolutedigitalpublishers.com/papers/quantum-relativity-03-frame-invariant-entanglement.pdf.

[19] R. Corgier, N. Gaaloul, A. Smerzi, L. Pezzè (2021). Delta-Kick Squeezing. *Physical Review Letters, vol. 127, article 183401*. https://arxiv.org/abs/2103.10896. DOI: 10.1103/PhysRevLett.127.183401.

[20] R. Corgier, M. Malitesta, A. Smerzi, L. Pezzè (2023). Quantum-enhanced differential atom interferometers and clocks with spin-squeezing swapping. *Quantum, vol. 7, article 965*. https://arxiv.org/abs/2205.09698. DOI: 10.22331/q-2023-03-30-965.

[21] T. Damour (2012). Theoretical Aspects of the Equivalence Principle. *Classical and Quantum Gravity, vol. 29, article 184001*. https://arxiv.org/abs/1202.6311. DOI: 10.1088/0264-9381/29/18/184001.

[22] T. Damour, J. F. Donoghue (2010). Equivalence Principle Violations and Couplings of a Light Dilaton. *Physical Review D, vol. 82, article 084033*. https://arxiv.org/abs/1007.2792.

[23] P. Delva, N. Puchades, E. Schönemann, F. Dilssner, C. Courde, S. Bertone, F. Gonzalez, A. Hees, Ch. Le Poncin-Lafitte, F. Meynadier, R. Prieto-Cerdeira, B. Sohet, J. Ventura-Traveset, P. Wolf (2018). Gravitational Redshift Test Using Eccentric Galileo Satellites. *Physical Review Letters, vol. 121, article 231101*. https://arxiv.org/abs/1812.03711. DOI: 10.1103/PhysRevLett.121.231101.

[24] L. Diósi (1984). Gravitation and quantum mechanical localization of macro-objects. *Physics Letters A, vol. 105, pp. 199–202*. https://arxiv.org/abs/1412.0201. DOI: 10.1016/0375-9601(84)90397-9.

[25] O. Dobkowski, B. Trok, P. Skakunenko, Y. Japha, D. Groswasser, M. Efremov, C. Marletto, I. Fuentes, R. Penrose, V. Vedral, W. P. Schleich, R. Folman (2025). Observation of quantum free fall and the consistency with the equivalence principle. *arXiv:2502.14535*. https://arxiv.org/abs/2502.14535.

[26] S. Donadi, K. Piscicchia, C. Curceanu, L. Diósi, M. Laubenstein, A. Bassi (2021). Underground test of gravity-related wave function collapse. *Nature Physics, vol. 17, pp. 74–78*. https://arxiv.org/abs/2111.13490.

[27] X.-C. Duan, M.-K. Zhou, X.-B. Deng, H.-B. Yao, C.-G. Shao, J. Luo, Z.-K. Hu (2016). Test of the Universality of Free Fall with Atoms in Different Spin Orientations. *Physical Review Letters, vol. 117, article 023001*. https://arxiv.org/abs/1503.00433. DOI: 10.1103/PhysRevLett.117.023001.

[28] V. A. Emelyanov (2022). On free fall of quantum matter. *European Physical Journal C, vol. 82, article 318*. https://arxiv.org/abs/2110.10056. DOI: 10.1140/epjc/s10052-022-10269-1.

[29] G. Fabiano, T. Fujita, A. Matsumura, D. Carney (2026). Minimal noise in non-quantized gravity. *arXiv:2603.26075*. https://arxiv.org/abs/2603.26075.

[30] M. Fadel, T. Zibold, B. Décamps, P. Treutlein (2018). Spatial entanglement patterns and Einstein-Podolsky-Rosen steering in Bose-Einstein condensates. *Science, vol. 360, pp. 409–413*. https://arxiv.org/abs/1708.02534. DOI: 10.1126/science.aao1850.

[31] P. Fayet (2019). MICROSCOPE limits on the strength of a new force, with comparisons to gravity and electromagnetism. *Physical Review D, vol. 99, article 055043*. https://arxiv.org/abs/1809.04991. DOI: 10.1103/PhysRevD.99.055043.

[32] S. Fray, C. Alvarez Diez, T. W. Hänsch, M. Weitz (2004). Atomic Interferometer with Amplitude Gratings of Light and Its Applications to Atom Based Tests of the Equivalence Principle. *Physical Review Letters, vol. 93, article 240404*. https://arxiv.org/abs/physics/0411052. DOI: 10.1103/PhysRevLett.93.240404.

[33] N. Gaaloul, H. Ahlers, L. Badurina, et al. (2022). STE-QUEST — Space Time Explorer and Quantum Equivalence Principle Space Test: The 2022 medium-class mission concept. *arXiv:2211.15412*. https://arxiv.org/abs/2211.15412.

[34] R. Geiger, M. Trupke (2018). Proposal for a Quantum Test of the Weak Equivalence Principle with Entangled Atomic Species. *Physical Review Letters, vol. 120, article 043602*. https://arxiv.org/abs/1801.08604. DOI: 10.1103/PhysRevLett.120.043602.

[35] N. Gisin (1990). Weinberg's non-linear quantum mechanics and supraluminal communications. *Physics Letters A, vol. 143, pp. 1–2*. DOI: 10.1016/0375-9601(90)90786-N.

[36] G. P. Greve, C. Luo, B. Wu, J. K. Thompson (2022). Entanglement-Enhanced Matter-Wave Interferometry in a High-Finesse Cavity. *Nature, vol. 610, pp. 472–477*. https://arxiv.org/abs/2110.14027. DOI: 10.1038/s41586-022-05197-9.

[37] A. Großardt, J. Bateman, H. Ulbricht, A. Bassi (2016). Optomechanical test of the Schrödinger-Newton equation. *Physical Review D, vol. 93, article 096003*. https://arxiv.org/abs/1510.01696.

[38] B. Helou, J. Luo, H.-C. Yeh, C.-g. Shao, B. J. J. Slagmolen, D. E. McClelland, Y. Chen (2017). Measurable signatures of quantum mechanics in a classical spacetime. *Physical Review D, vol. 96, article 044008*. https://arxiv.org/abs/1612.06310.

[39] S. Herrmann, F. Finke, M. Lülf, O. Kichakova, D. Puetzfeld, D. Knickmann, M. List, B. Rievers, G. Giorgi, C. Günther, H. Dittus, R. Prieto-Cerdeira, F. Dilssner, F. Gonzalez, E. Schönemann, J. Ventura-Traveset, C. Lämmerzahl (2018). Test of the Gravitational Redshift with Galileo Satellites in an Eccentric Orbit. *Physical Review Letters, vol. 121, article 231102*. https://arxiv.org/abs/1812.09161. DOI: 10.1103/PhysRevLett.121.231102.

[40] O. Hosten, N. J. Engelsen, R. Krishnakumar, M. A. Kasevich (2016). Measurement noise 100 times lower than the quantum-projection limit using entangled atoms. *Nature, vol. 529, pp. 505–508*. https://www.nature.com/articles/nature16176. DOI: 10.1038/nature16176.

[41] S. Huck et al. (AEgIS Collaboration) (2023). Toward a pulsed antihydrogen beam for WEP tests in AEgIS. *EPJ Web of Conferences, vol. 282, article 01005*. https://doi.org/10.1051/epjconf/202328201005. DOI: 10.1051/epjconf/202328201005.

[42] D. Kafri, J. M. Taylor, G. J. Milburn (2014). A classical channel model for gravitational decoherence. *New Journal of Physics, vol. 16, article 065020*. https://arxiv.org/abs/1401.0946.

[43] P. Kómár, E. M. Kessler, M. Bishof, L. Jiang, A. S. Sørensen, J. Ye, M. D. Lukin (2014). A quantum network of clocks. *Nature Physics, vol. 10, pp. 582–587.* https://arxiv.org/abs/1310.6045. DOI: 10.1038/nphys3000.

[44] P. Kunkel, M. Prüfer, H. Strobel, D. Linnemann, A. Frölian, T. Gasenzer, M. Gärttner, M. K. Oberthaler (2018). Spatially distributed multipartite entanglement enables Einstein-Podolsky-Rosen steering of atomic clouds. *Science, vol. 360, pp. 413–416.* https://arxiv.org/abs/1708.02407. DOI: 10.1126/science.aao2254.

[45] K. Lange, J. Peise, B. Lücke, I. Kruse, G. Vitagliano, I. Apellaniz, M. Kleinmann, G. Toth, C. Klempt (2018). Entanglement between two spatially separated atomic modes. *Science, vol. 360, pp. 416–418.* https://arxiv.org/abs/1708.02480. DOI: 10.1126/science.aao2035.

[46] B. K. Malia, Y. Wu, J. Martínez-Rincón, M. A. Kasevich (2022). Distributed quantum sensing with a mode-entangled network of spin-squeezed atomic states. *Nature, vol. 604, pp. 251–256.* https://arxiv.org/abs/2205.06382. DOI: 10.1038/s41586-022-05363-z.

[47] C. Marletto, V. Vedral (2017). Gravitationally-induced entanglement between two massive particles is sufficient evidence of quantum effects in gravity. *Physical Review Letters, vol. 119, article 240402.* https://arxiv.org/abs/1707.06036.

[48] C. Marletto, V. Vedral (2020). On the Testability of the Equivalence Principle as a Gauge Principle Detecting the Gravitational t^3 Phase. *Frontiers in Physics, vol. 8, article 176.* https://arxiv.org/abs/2004.11616. DOI: 10.3389/fphy.2020.00176.

[49] A. M. Nobili, D. Bramanti, E. Polacco, G. Catastini, A. Anselmi, S. Portigliotti, A. Lenti, A. Severi (2000). The 'Galileo Galilei' (GG) project: Testing the Equivalence Principle in space and on Earth. *Advances in Space Research, vol. 25, pp. 1231–1235.* https://doi.org/10.1016/S0273-1177(99)00992-8. DOI: 10.1016/S0273-1177(99)00992-8.

[50] A. M. Nobili, M. Shao, R. Pegna, G. Zavattini, S. G. Turyshev, D. M. Lucchesi, A. De Michele, S. Doravari, G. L. Comandi, T. R. Saravanan, F. Palmonari, G. Catastini, A. Anselmi (2012). 'Galileo Galilei' (GG): Space test of the weak equivalence principle to 10^{-17} and laboratory demonstrations. *Classical and Quantum Gravity, vol. 29, article 184011.* https://doi.org/10.1088/0264-9381/29/18/184011. DOI: 10.1088/0264-9381/29/18/184011.

[51] K. Nordtvedt (1968). Equivalence Principle for Massive Bodies. I. Phenomenology. *Physical Review, vol. 169, pp. 1014–1016.* DOI: 10.1103/PhysRev.169.1014.

[52] P. J. Orlando, R. B. Mann, K. Modi, F. A. Pollock (2016). A Simple Test of the Equivalence Principle(s) for Quantum Superpositions. *Classical and Quantum Gravity, vol. 33, article 19LT01.* https://arxiv.org/abs/1511.02943. DOI: 10.1088/0264-9381/33/19/19LT01.

[53] C. Overstreet, P. Asenbaum, T. Kovachy, R. Notermans, J. M. Hogan, M. A. Kasevich (2018). Effective Inertial Frame in an Atom Interferometric Test of the Equivalence Principle. *Physical Review Letters, vol. 120, article 183604.* https://arxiv.org/abs/1711.09986. DOI: 10.1103/PhysRevLett.120.183604.

[54] C. Overstreet, P. Asenbaum, J. Curti, M. Kim, M. A. Kasevich (2022). Observation of a gravitational Aharonov-Bohm effect. *Science, vol. 375, no. 6577, article abl7152.* https://doi.org/10.1126/science.abl7152. DOI: 10.1126/science.abl7152.

[55] E. Pedrozo-Peñafiel, S. Colombo, C. Shu, A. F. Adiyatullin, Z. Li, E. Mendez, B. Braverman, A. Kawasaki, D. Akamatsu, Y. Xiao, V. Vuletić (2020). Entanglement-Enhanced Optical Atomic Clock. *Nature, vol. 585, pp. 620–624.* https://arxiv.org/abs/2006.07501. DOI: 10.1038/s41586-020-3006-1.

[56] P. Perez, Y. Sacquin (GBAR Collaboration) (2012). The GBAR experiment: Gravitational behaviour of antihydrogen at rest. *Classical and Quantum Gravity, vol. 29, article 184008.* https://doi.org/10.1088/0264-9381/29/18/184008. DOI: 10.1088/0264-9381/29/18/184008.

[57] A. Peters, K. Y. Chung, S. Chu (1999). Measurement of gravitational acceleration by dropping atoms. *Nature, vol. 400, pp. 849–852.* DOI: 10.1038/23655.

[58] L. Pezzè, A. Smerzi, M. K. Oberthaler, R. Schmied, P. Treutlein (2018). Quantum metrology with nonclassical states of atomic ensembles. *Reviews of Modern Physics, vol. 90, article 035005.* https://arxiv.org/abs/1609.01609. DOI: 10.1103/RevModPhys.90.035005.

[59] I. Pikovski, M. Zych, F. Costa, Č. Brukner (2015). Universal decoherence due to gravitational time dilation. *Nature Physics, vol. 11, pp. 668–672.* https://arxiv.org/abs/1311.1095.

[60] J. Polchinski (1991). Weinberg's nonlinear quantum mechanics and the Einstein-Podolsky-Rosen

paradox. *Physical Review Letters, vol. 66, pp. 397–400*. DOI: 10.1103/PhysRevLett.66.397.

[61] G. Rosi, G. D'Amico, L. Cacciapuoti, F. Sorrentino, M. Prevedelli, M. Zych, Č. Brukner, G. M. Tino (2017). Quantum test of the equivalence principle for atoms in superpositions of internal energy eigenstates. *Nature Communications, vol. 8, article 15529*. https://arxiv.org/abs/1704.02296. DOI: 10.1038/ncomms15529.

[62] M. S. Safronova, D. Budker, D. DeMille, D. F. Jackson Kimball, A. Derevianko, C. W. Clark (2018). Search for New Physics with Atoms and Molecules. *Reviews of Modern Physics, vol. 90, article 025008*. https://arxiv.org/abs/1710.01833.

[63] L. Salvi, N. Poli, V. Vuletić, G. M. Tino (2018). Squeezing on momentum states for atom interferometry. *Physical Review Letters, vol. 120, article 033601*. https://arxiv.org/abs/1708.05112. DOI: 10.1103/PhysRevLett.120.033601.

[64] L. I. Schiff (1960). On Experimental Tests of the General Theory of Relativity. *American Journal of Physics, vol. 28, no. 4, p. 340*. DOI: 10.1119/1.1935800.

[65] S. Schlamminger, K.-Y. Choi, T. A. Wagner, J. H. Gundlach, E. G. Adelberger (2008). Test of the Equivalence Principle Using a Rotating Torsion Balance. *Physical Review Letters, vol. 100, article 041101*. https://arxiv.org/abs/0712.0607. DOI: 10.1103/PhysRevLett.100.041101.

[66] D. Schlippert, J. Hartwig, H. Albers, L. L. Richardson, C. Schubert, A. Roura, W. P. Schleich, W. Ertmer, E. M. Rasel (2014). Quantum Test of the Universality of Free Fall. *Physical Review Letters, vol. 112, article 203002*. https://arxiv.org/abs/1406.4979. DOI: 10.1103/PhysRevLett.112.203002.

[67] C. Schubert, J. Hartwig, H. Ahlers, K. Posso-Trujillo, N. Gaaloul, U. Velte, A. Landragin, A. Bertoldi, B. Battelier, P. Bouyer, F. Sorrentino, G. M. Tino, M. Krutzik, A. Peters, S. Herrmann, C. Lämmerzahl, L. Cacciapuoti, E. Rocco, K. Bongs, W. Ertmer, E. M. Rasel (2013). Differential atom interferometry with ^{87}Rb and ^{85}Rb for testing the UFF in STE-QUEST. *arXiv:1312.5963*. https://arxiv.org/abs/1312.5963.

[68] M. Schulte, C. Lisdat, P. O. Schmidt, U. Sterr, K. Hammerer (2020). Prospects and challenges for squeezing-enhanced optical atomic clocks. *Nature Communications, vol. 11, article 5955*. https://arxiv.org/abs/1911.00882. DOI: 10.1038/s41467-020-19403-7.

[69] L. Seveso, M. G. A. Paris (2017). Can quantum probes satisfy the weak equivalence principle? *Annals of Physics, vol. 380, pp. 213–223*. https://arxiv.org/abs/1612.07331. DOI: 10.1016/j.aop.2017.03.021.

[70] W. Struyve (2025). Absence of gravitationally induced entanglement in certain semi-classical theories of gravity. *arXiv:2510.20991*. https://arxiv.org/abs/2510.20991.

[71] T. J. Sumner, J. Anderson, J.-P. Blaser, A. M. Cruise, T. Damour, et al. (2007). STEP (satellite test of the equivalence principle). *Advances in Space Research, vol. 39, pp. 254–258*. https://doi.org/10.1016/j.asr.2006.09.019. DOI: 10.1016/j.asr.2006.09.019.

[72] S. S. Szigeti, O. Hosten, S. A. Haine (2020). Improving cold-atom sensors with quantum entanglement: Prospects and challenges. *Applied Physics Letters, vol. 118, article 140501*. https://arxiv.org/abs/2010.09168. DOI: 10.1063/5.0050235.

[73] M. Takamoto, I. Ushijima, N. Ohmae, T. Yahagi, K. Kokado, H. Shinkai, H. Katori (2020). Test of general relativity by a pair of transportable optical lattice clocks. *Nature Photonics, vol. 14, pp. 411–415*. https://doi.org/10.1038/s41566-020-0619-8. DOI: 10.1038/s41566-020-0619-8.

[74] M. G. Tarallo, T. Mazzoni, N. Poli, D. V. Sutyrin, X. Zhang, G. M. Tino (2014). Test of Einstein Equivalence Principle for 0-spin and half-integer-spin atoms: Search for spin-gravity coupling effects. *Physical Review Letters, vol. 113, article 023005*. https://arxiv.org/abs/1403.1161. DOI: 10.1103/PhysRevLett.113.023005.

[75] A. Tilloy, L. Diósi (2016). Sourcing semiclassical gravity from spontaneously localized quantum matter. *Physical Review D, vol. 93, article 024026*. https://arxiv.org/abs/1509.08705.

[76] P. Touboul et al. (2017). The MICROSCOPE mission: first results of a space test of the Equivalence Principle. *Physical Review Letters, vol. 119, article 231101*. https://arxiv.org/abs/1712.01176. DOI: 10.1103/PhysRevLett.119.231101.

[77] P. Touboul et al. (2022). MICROSCOPE Mission: Final Results of the Test of the Equivalence Principle. *Physical Review Letters, vol. 129, article 121102*. https://arxiv.org/abs/2209.15487. DOI: 10.1103/PhysRevLett.129.121102.

[78] P. Touboul et al. (2022). Result of the MICROSCOPE weak equivalence principle test. *Classical and Quantum Gravity, vol. 39, arti-*

cle 204009. https://arxiv.org/abs/2209.15488. DOI: 10.1088/1361-6382/ac84be.

[79] D. Trillo, M. Navascués (2024). The Diósi-Penrose model of classical gravity predicts gravitationally induced entanglement. *Physical Review D, vol. 111, article L121101 (2025)*. https://arxiv.org/abs/2411.02287.

[80] R. F. C. Vessot, M. W. Levine, E. M. Mattison, E. L. Blomberg, T. E. Hoffman, et al. (1980). Test of Relativistic Gravitation with a Space-Borne Hydrogen Maser. *Physical Review Letters, vol. 45, pp. 2081–2084*. DOI: 10.1103/PhysRevLett.45.2081.

[81] V. Viswanathan, A. Fienga, O. Minazzoli, L. Bernus, J. Laskar, M. Gastineau (2018). The new lunar ephemeris INPOP17a and its application to fundamental physics. *Monthly Notices of the Royal Astronomical Society, vol. 476, pp. 1877–1888*. https://arxiv.org/abs/1710.09167. DOI: 10.1093/mnras/sty096.

[82] T. A. Wagner, S. Schlamminger, J. H. Gundlach, E. G. Adelberger (2012). Torsion-balance tests of the weak equivalence principle. *Classical and Quantum Gravity, vol. 29, article 184002*. https://arxiv.org/abs/1207.2442. DOI: 10.1088/0264-9381/29/18/184002.

[83] S. Weinberg (1989). Testing Quantum Mechanics. *Annals of Physics, vol. 194, pp. 336–386*. DOI: 10.1016/0003-4916(89)90276-5.

[84] C. M. Will (2014). The Confrontation between General Relativity and Experiment. *Living Reviews in Relativity, vol. 17, article 4*. https://arxiv.org/abs/1403.7377.

[85] J. G. Williams, S. G. Turyshev, D. H. Boggs (2004). Progress in Lunar Laser Ranging Tests of Relativistic Gravity. *Physical Review Letters, vol. 93, article 261101*. https://arxiv.org/abs/gr-qc/0411113. DOI: 10.1103/PhysRevLett.93.261101.

[86] H. Yang, H. Miao, D.-S. Lee, B. Helou, Y. Chen (2013). Macroscopic Quantum Mechanics in a Classical Spacetime. *Physical Review Letters, vol. 110, article 170401*. https://arxiv.org/abs/1210.0457.

[87] L. Zhou, S. Long, B. Tang, X. Chen, F. Gao, W. Peng, W. Duan, J. Zhong, Z. Xiong, J. Wang, Y. Zhang, M. Zhan (2015). Test of Equivalence Principle at 10^{-8} Level by a Dual-species Double-diffraction Raman Atom Interferometer. *Physical Review Letters, vol. 115, article 013004*. https://arxiv.org/abs/1503.00401. DOI: 10.1103/PhysRevLett.115.013004.

[88] M. Zych, Č. Brukner (2018). Quantum formulation of the Einstein Equivalence Principle. *Nature Physics, vol. 14, pp. 1027–1031*. https://arxiv.org/abs/1502.00971. DOI: 10.1038/s41567-018-0197-6.

[89] M. Zych, F. Costa, I. Pikovski, Č. Brukner (2011). Quantum interferometric visibility as a witness of general relativistic proper time. *Nature Communications, vol. 2, article 505*. https://arxiv.org/abs/1105.4531.